Structures of *N*-Glycans of a Ricin-Resistant Mutant of Baby Hamster Kidney Cells. Synthesis of High-Mannose and Hybrid *N*-Glycans†

Paul A. Gleeson,‡ James Feeney, and R. Colin Hughes*

National Institute for Medical Research, Mill Hill, London NW7 1AA, United Kingdom
Received May 8, 1984

ABSTRACT: The asparagine-linked glycopeptides (*N*-glycans) of a ricin-resistant mutant of baby hamster kidney (BHK) cells, Ric^{R}21, have been isolated and fractionated from a Pronase digest of disrupted cells by concanavalin A (Con A)–Sepharose chromatography, ion-exchange chromatography, and lentil lectin chromatography. The structures of all the major *N*-glycans have been determined by 500-MHz ^{1}H NMR spectroscopy. Ric^{R}21 synthesizes only hybrid and high-mannose *N*-glycans. All the hybrid structures contain only three mannose residues. The major hybrid glycopeptide has the following structure:

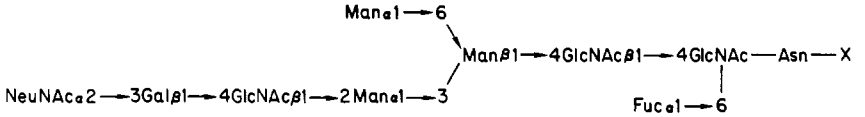

There is also about 15% of the nonfucosylated species present. Only a small amount (≤5%) of the asialo hybrid is produced. Branched hybrid *N*-glycans are also present in Ric^{R}21 cells, containing two complex antenna linked β1→2 and β1→4 to the Man α1→3 arm; about 70% of this species is core fucosylated. $Man_6GlcNAc_2$ glycopeptide is the most abundant (about 70%) of the high-mannose *N*-glycans. These studies account for the very poor ricin binding property of this mutant, as the sialic acid residues of the major hybrid *N*-glycan are exclusively linked α2→3 to galactose and ricin is unable to bind to α2→3-substituted galactosyl residues [Baenziger, J. U., & Fiete, D. (1979) *J. Biol. Chem. 254*, 9795–9799].

Previous work from this laboratory has shown that the glycoproteins present in ricin-resistant mutants of baby hamster kidney (BHK) cells carry asparagine-linked carbohydrate units (*N*-glycans) with altered composition compared with the *N*-glycans of the ricin-sensitive parental cells (Hughes & Mills, 1983; Hughes et al., 1983). Major glycopeptide fractions were obtained from the cells by Pronase digestion followed by affinity chromatography on concanavalin A–Sepharose. In general, an increased proportion of glycopeptides binding with high affinity to the Con A–Sepharose[1] column was obtained for the ricin-resistant mutants. Since concanavalin A shows low affinity for complex tri- and tetraantennary *N*-glycans and biantennary *N*-glycans of the form

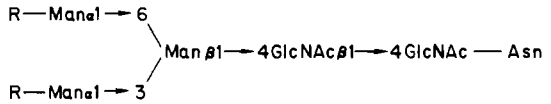

where R is [±NeuNAcα2→3(6)]Galβ1→4GlcNAcβ1→2 (Ogata et al., 1975; Krusius et al., 1976; Narasimhan et al., 1979), these observations were consistent with a generalized block in the mutants in conversion of high-mannose *N*-glycans to complex *N*-glycans. Ricin binds to complex *N*-glycans (Baenziger & Fiete, 1979), and hence, these alterations in carbohydrate structure explain in general the failure of the mutants to bind ricin and increased resistance to the cytotoxicity of the lectin (Meager et al., 1976; Rosen & Hughes, 1977; Finne & Krusius, 1982).

This paper describes an analysis of the *N*-glycans of one ricin-resistant BHK cell line, Ric^{R}21. Glycopeptides from Pronase-digested cells were fractionated by lectin affinity chromatography and ion-exchange chromatography, and their structures have been established definitively by high-resolution proton NMR spectroscopy at 500 MHz. The findings confirm and extend our earlier results (Hughes & Mills, 1983; Hughes et al., 1983) and for the first time provide a description of the major *N*-glycan structures present in a particular cell type from NMR spectroscopy.

Experimental Procedures

Materials

Bio-Gel P-2 (100–200 mesh), Bio-Gel P-10 (100–200 mesh), and Chelex 100 (100–200 mesh, Na^+ form) were purchased from Bio-Rad Laboratories. Concanavalin A (Con A)–Sepharose 4B and lentil lectin–Sepharose 4B were obtained from Pharmacia. [1-^{14}C]Acetic anhydride (10.0 mCi/mmol) was from New England Nuclear. D-[2-^{3}H]mannose (13.4 Ci/mmol) and 2-amino-2-deoxy-D-[1-^{14}C]glucose hydrochloride (56.8 mCi/mmol) were from Amersham International, U.K. Deuterum oxide (99.8 and 99.996%) was from Aldrich. *Vibro cholerae* neuraminidase (1 IU/mL) and Pronase CB were purchased from Calbiochem-Behring Corp., and the endo-β-*N*-acetylglucosaminidase D and endo-β-*N*-acetylglucosaminidase H were from Miles Laboratories. Bovine pancreatic deoxyribonuclease I (2350 Kunitz units/mg) was obtained from Sigma. The $Man_5GlcNAc_2Asn$ glycopeptide, prepared from ovalbumin by the method of Narasimhan et al. (1980), was a gift from Dr. H. Schachter and S. Allen.

Methods

Cells. Baby hamster kidney (BHK) C13 cells and ricin-resistant cell line Ric^{R}21 (Meager et al., 1976) were grown

† P.G. is supported by a Beit Memorial Medical Fellowship.
‡ Present address: Department of Biochemistry, La Trobe University, Bundoora, Victoria, Australia 3083.

[1] Abbreviations: Con A, concanavalin A; EDTA, ethylenediaminetetraacetic acid; Tris-HCl, tris(hydroxymethyl)aminomethane hydrochloride.

0006-2960/85/0424-0493$01.50/0

in Glasgow-modified Eagle's medium supplemented with 10% fetal calf serum at 37 °C as described by Meager et al. (1976). For large-scale growth, the Ric^{R}21 cells were grown in 18 roller bottles (800 cm^2) to confluency and the monolayers washed twice with phosphate-buffered saline, pH 7.2, containing 5 mM EDTA (Hughes et al., 1983) and harvested by scraping with a rubber policeman in the same buffer. The cells were pelleted at 800*g* for 10 min and washed once with phosphate-buffered saline, pH 7.2, without EDTA. The total yield was (5–10) × 10^9 cells. Ric^{R}21 cells were also labeled metabolically by growth for 3 days at 37 °C in the medium containing 20 μCi/mL D-[2-^{3}H]mannose or 5 μCi/mL D-[1-^{14}C]glucosamine in 100-mm diameter tissue culture plates as previously described (Hughes et al., 1983). The ^{14}C- and ^{3}H-labeled cells were combined with the packed unlabeled cells.

Isolation of Cellular Glycopeptides. Frozen washed pellets were thawed and extracted with 200 mL of chloroform/methanol (2:1) at room temperature for 2 h to remove glycolipids, and the residue was recovered by centrifugation at 2000*g* for 10 min. The extraction was repeated a second time and the residue finally washed with ethanol. The delipidated residue was suspended in 60 mL of 0.1 M Tris-HCl, pH 8.0, containing 5 mM $CaCl_2$ and 0.02% sodium azide, and placed in a boiling water bath for 6 min. After this was cooled to 37 °C, Pronase was added (30 mg at zero time and 30 mg each at 24 and 48 h) and incubated for 72 h at 37 °C. Before each addition of Pronase, the pH was readjusted to pH 8.0 with 1 N NaOH. The digest was then treated at 100 °C for 6 min to stop the reaction and after being cooled was incubated with 0.002 mg/mL (4.7 units/mg) of bovine pancreatic DNase I at 37 °C for 1 h to reduce the viscosity. The reaction was stopped by boiling for 6 min. The digest was then centrifuged at 12000*g* for 15 min and the residue subjected to a second Pronase digestion. In all, 90–100% of the total radioactivity present in the cell pellet was recovered in the supernatant. Polyanionic material (DNA and glycosaminoglycans) was removed from the digest by precipitation with cetylpyridinium chloride as described by Finne & Krusius (1982). Briefly, 10 mL (0.1 volume) of 0.1 M cetylpyridinium chloride, containing 0.1 M sodium sulfate, was added dropwise to the digest and kept at 37 °C for 20 min. The precipitate was removed by centrifugation at 15000*g* for 15 min. The supernatant was then cooled to 4 °C, and the excess cetylpyridinium chloride was removed by addition of 11 mL (0.1 volume) of 0.1 M potassium thiocyanate, kept at 4 °C overnight, and finally centrifuged at 20000*g* for 30 min. Approximately 8.3% of the total ^{14}C radioactivity and 6.0% of the ^{3}H radioactivity were precipitated by this treatment.

Half of the resultant supernatant (60 mL) was applied to a Sephadex G-25 column (4 × 112 cm), and the column was eluted in water containing 0.02% sodium azide at room temperature to isolate the glycopeptides. Fractions of 7 mL were collected, and a single major peak (fractions 60–100) was obtained containing both the ^{14}C (84%) and ^{3}H (97%) radiolabels. There was also a minor peak eluting with a lower molecular weight (fractions 105–140) which contained only ^{14}C radioactivity, and presumably represents low molecular weight *O*-glycans.

Fractionation of Ric^{R}21 Glycopeptides. The scheme for the fraction of the glycopeptides is depicted in Figure 1.

(*A*) *Con A–Sepharose Chromatography.* The major peak from the Sephadex G-25 column was pooled and concentrated to 6 mL by rotary evaporation. Aliquots (3 mL, containing 1.5 μmol of glycopeptide, as determined by neutral sugar assay) were applied to a column (0.9 × 51 cm) of Con A–Sepharose (Pharmacia), equilibrated in 10 mM Tris-HCl, pH 7.5, containing 0.1 M NaCl, 1 mM $MgCl_2$, 1 mM $CaCl_2$, 1 mM $MnCl_2$, and 0.02% sodium azide. Chromatography was performed at room temperature with a flow rate of 16 mL/h, and 2-mL fractions were collected. The column was washed with 80 mL of the starting buffer followed by 60 mL of the buffer containing 10 mM methyl α-D-glucoside followed by 60 mL of the buffer containing 100 mM methyl α-D-mannoside. Aliquots (20 μL) were counted for radioactivity. Approximately 60% of the total radioactivity applied to the column was recovered. The elution profile is shown in Figure 2. The bound fraction and the unbound fraction containing both ^{14}C and ^{3}H radiolabels were pooled as indicated, dried on a rotary evaporator, and desalted on a column (2 × 26.5 cm) of Bio-Gel P-2. There was also an additional unbound fraction, highly enriched in the ^{14}C radiolabel, that eluted earlier than the ^{14}C/^{3}H-labeled unbound fraction. This material presumably represents large molecular weight *O*-glycans and was not further investigated.

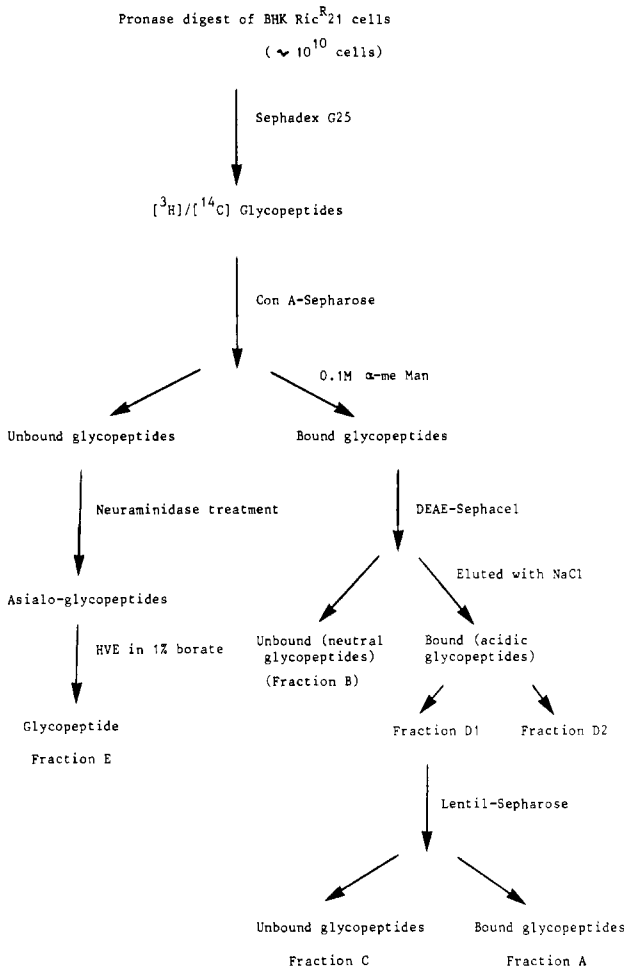

FIGURE 1: Fractionation scheme of Ric^{R}21 glycopeptides. Glycopeptides were obtained by pooling unlabeled cells with cells grown in medium containing D-[2-^{3}H]mannose or D-[1-^{14}C]glucosamine.

(*B*) *DEAE-Sephacel Chromatography.* The Con A bound glycopeptides were further fractionated by ion-exchange chromatography on a column (1.1 × 17 cm) of DEAE-Sephacel, as described previously (Hughes et al., 1983). The column was initially equilibrated with 50 mM acetic acid at 2 °C, the glycopeptide sample in water (2 mL) was applied to the column, and the column flow was stopped for 1 h. The column was then washed with water at a flow rate of 8 mL/h, and 1-mL fractions were collected. After collection of 24 fractions, the bound glycopeptides were eluted with a linear

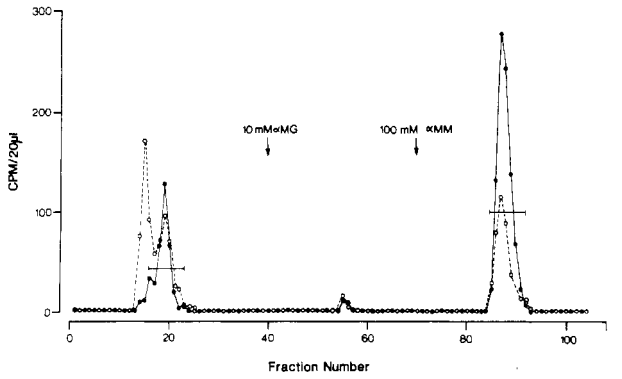

FIGURE 2: Chromatography of Ric^{R}21 glycopeptides on Con A–Sepharose. $^3H/^{14}C$ labeled Ric^{R}21 glycopeptides (approximately 1.5 µmol) from the Sephadex G-25 column were applied to a column (0.9 × 51 cm) of Con A–Sepharose equilibrated and eluted at room temperature with 10 mM Tris-HCl, pH 7.5, containing 0.1 M NaCl, 1 mM $MnCl_2$, 1 mM $MgCl_2$, 1 mM $CaCl_2$, and 0.02% sodium azide. The arrows indicate the start of elution with 10 mM methyl α-D-glucoside (αMG) and 100 mM methyl α-D-mannoside (αMM), respectively. Fractions of 2 mL were collected, and 20-µL aliquots were removed for counting: ^3H radioactivity; (○) ^{14}C radioactivity. Fractions were pooled as indicated.

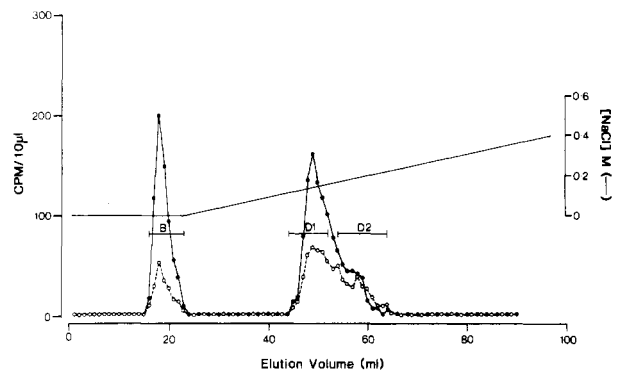

FIGURE 3: Ion-exchange chromatography of Con A bound Ric^{R}21 glycopeptides on DEAE-Sephacel. The $^3H/^{14}C$ labeled Con A bound Ric^{21} glycopeptides (Figure 2) in 2 mL of water were applied to a DEAE-Sephacel column (1.1 × 17 cm) equilibrated in 50 mM acetic acid, as described under Methods. A sodium chloride gradient was applied at fraction 23, as indicated, to elute the bound glycopeptides. Flow rate was 8 mL/h, 1-mL fractions were collected, and 10-µL aliquots were removed for counting: (●) ^3H radioactivity; (○) ^{14}C radioactivity. Fractions were pooled as indicated.

salt gradient of 0.0–0.5 M NaCl (45 and 45 mL) in 50 mM acetic acid. Aliquots of 10 µL were counted for radioactivity. Approximately 95% of the total radioactivity applied was recovered from the column. The elution profile is shown in Figure 3; fractions were pooled as indicated, freeze-dried, and desalted on a column (2 × 26.5 cm) of Bio-Gel P-2.

(C) Lentil–Sepharose Chromatography. The major peak of the DEAE-bound fraction (fraction D1, Figure 3) was fractionated on a column (0.9 × 12 cm) of lentil lectin–Sepharose (Pharmacia) at room temperature, equilibrated in 10 mM Tris-HCl, pH 7.5, containing 0.1 M NaCl, 1 mM $MgCl_2$, 1 mM $MnCl_2$, 1 mM $CaCl_2$, and 0.02% sodium azide. The glycopeptide sample (in 1 mL of the above buffer) was loaded onto the column and the column washed with 30 mL of the above buffer followed by 20 mL of the buffer containing 200 mM methyl α-D-mannoside. Greater than 90% of the total radioactivity applied was recovered from the column. The bound and unbound fractions were pooled as indicated (Figure 4) and desalted on the Bio-Gel P-2 column. Analytical chromatography on lentil lectin–Sepharose was performed as described above, except that samples (150–200 µL) were loaded onto the column, which was then washed with 25 mL

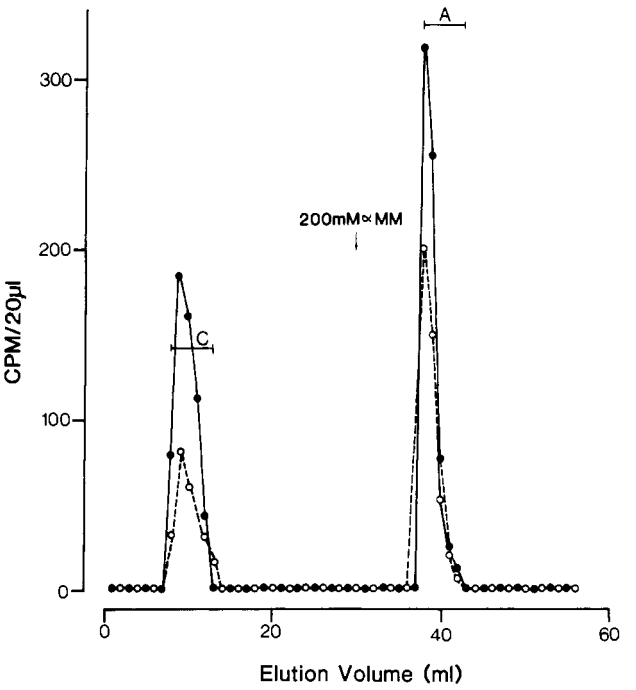

FIGURE 4: Chromatography of Ric^{R}21 DEAE-Sephacel-bound glycopeptides (fraction D1) on lentil lectin–Sepharose. The $^3H/^{14}C$ glycopeptide fraction D1 (in 1 mL) was applied to a column (0.9 × 12 cm) of lentil lectin–Sepharose equilibrated and eluted at room temperature in 10 mM Tris-HCl, pH 7.5, containing 0.1 M NaCl, 1 mM $MnCl_2$, 1 mM $MgCl_2$, 1 mM $CaCl_2$, and 0.02% sodium azide. The arrow indicates the start of elution with 200 mM methyl α-D-mannoside (αMM). Fractions of 1 mL were collected, and 20-µL aliquots were removed for counting: (●) ^3H radioactivity; (○) ^{14}C radioactivity. Fractions were pooled as indicated.

of buffer followed by 28 mL of buffer containing 10 mM methyl α-D-glucoside and finally 25 mL of buffer containing 200 mM methyl α-D-mannoside.

Con A Unbound Glycopeptides. The pooled Con A unbound fraction (Figure 2) was dissolved in 2 mL of 50 mM sodium acetate buffer, pH 5.5, containing 9 mM $CaCl_2$, 0.154 M NaCl, and 0.02% sodium azide and treated with 0.2 unit of *V. cholerae* neuraminidase for 48 h at 37 °C to remove the sialic acid residues. The reaction was stopped by heating it at 100 °C for 10 min and the digest then chromatographed on a column (1.6 × 97 cm) of Bio-Gel P-10 (100–200 mesh) equilibrated in 0.1 M NaCl to separate the released sialic acid (fractions 110–125) from the glycopeptides (fractions 75–100). The $^3H/^{14}C$-labeled glycopeptide peak was pooled, dried on a rotary evaporator, and desalted on the Bio-Gel P-2 column. The sample was then subjected to high-voltage electrophoresis in 1% sodium borate, as described below.

High-Voltage Electrophoresis in 1% Sodium Borate. Preparative high-voltage electrophoresis was carried out as described by Narasimhan et al. (1980). The radioactive sample (in 100 µL of water) was spotted across 25 cm of Whatman 3MM paper, the paper being moistened with 1% aqueous sodium tetraborate, and subjected to high-voltage electrophoresis in 1% sodium tetraborate, pH 9.1, at 54 V/cm for 3 h 35 min, after which the marker dye 2,6-dichlorophenolindophenol (Sigma) had migrated 30 cm from the origin. The chromatogram was scanned with a radiochromatogram scanner, and the single major glycopeptide peak was eluted with water. The sample was dried on a rotary evaporator and the borate removed as the methyl ester by drying the sample 6 times with 10 mL of methanol/1% acetic acid.

Glycosidase Digestions. Treatment with endo-β-*N*-acetylglucosaminidase D was carried out in 100 µL of 0.15

M sodium phosphate buffer, pH 6.5, with 10 milliunits of endo D for 16 h at 37 °C. Treatment with endo-β-*N*-acetylglucosaminidase H was carried out in 100 μL of 0.1 M sodium citrate buffer, pH 5.5, with 10 milliunits of endo H for 16 h at 37 °C.

The reactions were stopped by boiling for 5 min, and the products were analyzed by chromatography on a Con A–Sepharose column (0.7 × 4 cm) under similar conditions as described earlier. Fractions of 1 mL were collected directly into scintillation vials, and after the column was washed with 10 mL of the pH 7.5 buffer, the bound material was eluted by washing the column with 10 mL of 100 mM methyl α-D-mannoside in the pH 7.5 buffer.

Control endoglycosidase digestions were also carried out with N-[^{14}C]acetylated $Man_5GlcNAc_2$ glycopeptide and the products analyzed in a similar manner on Con A–Sepharose. The glycopeptide was N-acetylated with [1-^{14}C]acetic anhydride as described by Narasimhan (1982).

Nuclear Magnetic Resonance (NMR) Spectroscopy. Samples (50–150 nmol) were prepared for proton NMR analyses by removing heavy metal ions by chromatography on a column (0.7 × 7 cm) of Chelex 100 (200–400 mesh) (Na^+ form) that had been washed with water. Samples were dried by rotary evaporation, transferred to small tubes, and exchanged 3 times from 99.8% deuterium oxide (Aldrich) (0.8 mL); drying was by rotary evaporation. Samples were then dissolved in 0.8 mL of 99.8% deuterium oxide and dried in an evacuated desiccator over phosphorus pentoxide for 48 h. The samples were removed and dissolved in 400 μL of 99.996% deuterium oxide (Aldrich) containing 4 mM acetone (internal reference) immediately prior to NMR analysis.

^{1}H NMR (500-MHz) spectra were measured at 22 and 70 °C in a Bruker AM500 NMR spectrometer operating in the Fourier-transform mode. The spectra were obtained by using quadrature detection with a spectral width of 6 kHz (or 8 kHz) and pulse intervals of up to 2.66 s. Most of the data were collected with 32K data points. Typically, 500–1000 transients were averaged, and before Fourier transformation, the free-induction decay was multiplied by an exponential function to improve sensitivity (giving an additional line broadening of 0.5 Hz). The chemical shifts were measured in ppm from an internal reference signal and expressed relative to DSS (4,4-dimethyl-4-silapentanesulfonate) by addition of 2.225 ppm.

Other Procedures. For amino acid and hexosamine analysis on a Beckman 121MB analyzer, samples were hydrolyzed with 4 N HCl for 4 h at 100 °C, under nitrogen, with 20 nmol of norleucine as internal standard. Liquid scintillation counting was carried out with EP (Beckman) scintillant in a Beckman LS 7000 counter. Neutral sugars were quantitated by the phenol–sulfuric acid assay (Dubois et al., 1956).

Results

Fractionation of Glycopeptides from BHK Ric^{R}21 Cells. The glycopeptides were obtained by Pronase digestion of delipidated cells (~10^{10}), as described under Methods. The fractionation scheme employed is outlined in Figure 1. Con A–Sepharose chromatography of the glycopeptides resulted in two major fractions, an unbound fraction and a fraction eluting with 100 mM methyl α-D-mannoside (Figure 2). Consistent with previous findings (Hughes et al., 1983), there was very little material that eluted in the presence of 10 mM methyl α-D-glucoside, indicating at best a very low content of complex biantennary *N*-glycans, in contrast to wild-type cells (Hughes et al., 1983).

Con A Bound Ric^{R}21 N-Glycans. The Con A–Sepharose-bound glycopeptides were further fractionated (Figure 1) on a DEAE-Sephacel column (Figure 3) and a lentil lectin–Sepharose column (Figure 4) to separate sialylated glycopeptides from high-mannose and other neutral species. Four fractions were obtained.

(*A*) *Glycopeptide Fraction A.* This fraction bound to both the DEAE-Sephacel (Figure 3) and lentil–Sepharose (Figure 4) columns and represents 28% of the ^{14}C radioactivity and 18% of the ^{3}H radioactivity of the total Con A bound material. Analysis after acid hydrolysis showed the following composition (molar ratio): $Asp_{1.00}Ser_{0.41}Thr_{0.56}Glu_{0.29}Gly_{0.51}Ala_{0.37}Val_{0.08}Met_{0.06}Leu_{0.07}Lys_{0.04}GlcNH_{3.35}$. Presumably, this fraction contains sialylated, fucosylated hybrid glycopeptides.

(*B*) *Glycopeptide Fraction B.* This fraction contains high-mannose glycopeptides, and any other neutral species, that did not absorb onto the DEAE-Sephacel column (Figure 3). This fraction represents 21.4% of the total ^{14}C radioactivity and 37% of the total ^{3}H radioactivity of the Con A bound fraction.

(*C*) *Glycopeptide Fraction C.* This fraction bound to the DEAE column but was unbound on lentil–Sepharose (Figure 4) and represents 10.7% of the ^{14}C radioactivity and 13.8% of the ^{3}H radioactivity of the total Con A bound fraction.

(*D*) *Glycopeptide Fraction D2.* This fraction eluted as a trailing shoulder from the main peak of the DEAE-bound fraction (Figure 3) and represents 30% of the ^{14}C radioactivity and 19.6% of the ^{3}H radioactivity of the total Con A bound fraction.

Structure of Ric^{R}21 Fraction A Glycopeptide. Glycopeptide fraction A was examined by proton NMR spectroscopy at 500 MHz. The spectrum, at 70 °C, is shown in Figure 5, and the chemical shifts obtained at both 22 and 70 °C are shown in Table I; assignments of the resonances throughout this paper are based on the published data of Vliegenthart et al. (1983), Carver et al. (1981), and Grey et al. (1982). The ratios of the intensity of the resolved anomeric proton resonances were integral, indicating that these correspond to a single major component (glycopeptide A) in this fraction. These anomeric hydrogen signals can be assigned as follows (Table I): Manα1→3 at 5.118 ppm, a broad peak due to Asn-linked GlcNAc at 5.057 ppm, Manα1→6 at 4.917 ppm, Fucα1→6 at 4.870 ppm, Manβ1→4 at 4.771 ppm (70 °C), a core GlcNAc doublet ($J_{1,2}$ = 8.8 Hz, indicating a β-linkage) at 4.683 ppm, GlcNAcβ1→2 at 4.571 ppm ($J_{1,2}$ = 7.8 Hz), and Galβ1→4 at 4.548 ppm ($J_{1,2}$ = 8.0 Hz). The chemical shifts of the *N*-acetyl groups are upfield with the *N*-acetyl groups of Asn-linked GlcNAc and core GlcNAc at 2.011 and 2.090 ppm, respectively, an *N*-acetyl group at 2.048 ppm due to an antennary (arm) GlcNAc residue, and an *N*-acetyl group at 2.030 ppm due to a sialic acid residue. Glycopeptide A, therefore, contains three mannose residues and only a single Galβ1→4GlcNAcβ1→2 antenna is present as the H-1 signals of galactose and arm GlcNAc each integrate to one hydrogen, and only a single *N*-acetyl group due to an arm GlcNAc is present at 2.048 ppm. Comparison of the H-1 and H-2 chemical shifts of the three mannose residues of glycopeptide A with those published by Grey et al. (1982) for the glycopeptides MM,[2] MG, and GM shows that the single *N*-acetyllactosamine branch is attached to the Manα1→3 residue. Glycopeptide A shows downfield shifts for the H-1 signal

[2] N-Linked glycopeptides are named according to the sugars present at the nonreducing termini of the antennae with the following code: Gn, GlcNAc; M, Man; G, Gal; S, sialic acid residue. The terminus on the Manα1→6 arm is named first followed by the terminus on the Manα1→3 arm. The presence of a core fucose is designated by (+F) (Narasimhan et al., 1979).

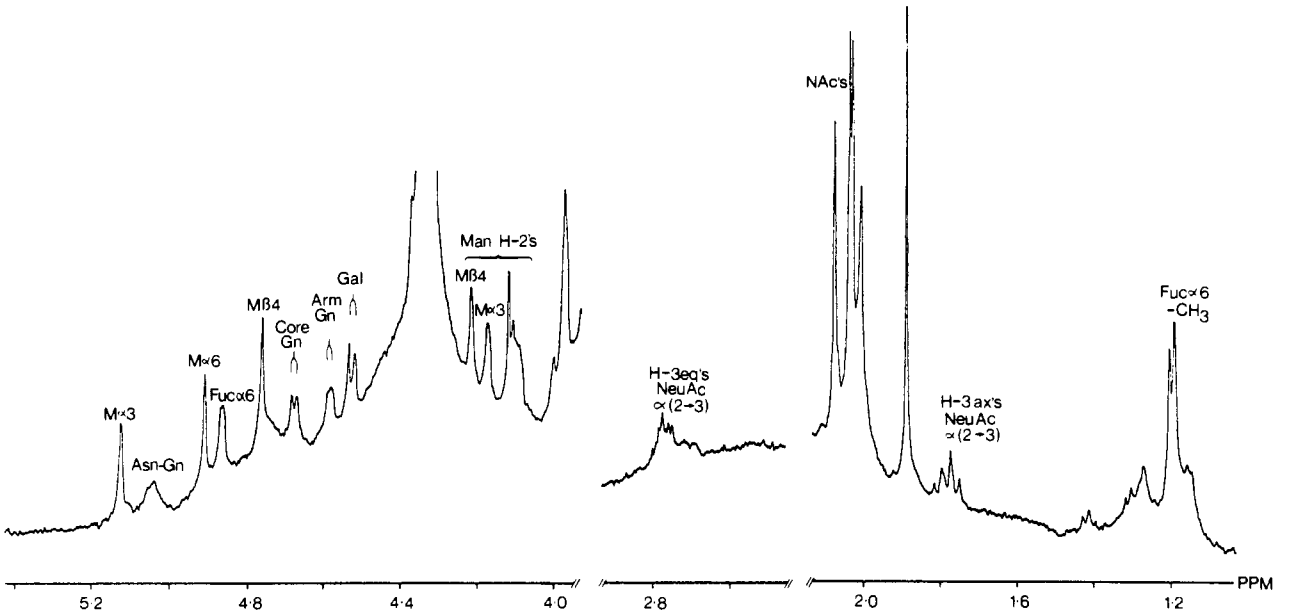

FIGURE 5: The 500-MHz ^1H NMR spectrum of Ric^R21 glycopeptide fraction A at 70 °C.

Table I: Chemical Shifts (ppm) of Glycopeptide Protons Derived from High-Resolution Proton NMR Spectroscopy at 500 MHz

	glycopeptide A		glycopeptide E		glycopeptide GGG[e]
protons	22 °C	70 °C	22 °C	70 °C	22 °C
H-1 of Man					
β1→4	*a*	4.771	4.769	4.760	4.755
α1→3	5.118	5.138	5.114	5.128	5.120
α1→6	4.917	4.921	4.915	4.917	4.924
H-2 of Man					
β1→4	4.256	4.229	4.220	4.201	4.209
α1→3	4.193	4.185	4.220	4.201	4.218
α1→6	?	?	<4.0	<4.0	4.108
H-1 of GlcNAc[b]					
I	4.571 (7.8)[c]	4.599	4.564 (8)	4.583	4.570
II					4.580
IV			4.542 (8)	4.583	4.545
V	5.057	5.057	5.057	5.056	5.092
VI	4.683 (8.8)	4.687	4.681 (8.8)	4.686 (4.622)[d]	4.614
H-1 of Gal[b]					
1	4.548 (8.0)	4.538	4.469 (8)	4.474	4.468
2					4.473
3			4.466 (8)	4.474	4.462
H-3 of Gal	4.089–4.129	4.095–4.133			
H-3 of Manα1→3			4.044	4.048	4.045
H-1 of Fuc	4.870 (3.8)	4.874	4.853	4.873	
H-5 of Fuc	4.089–4.129	4.095–4.133	4.136		
$-CH_3$ of Fuc	1.200	1.206	1.211	1.208	
H-3(a) of NeuNAc	1.799	1.783			
H-3(e) of NeuNAc	2.756	2.769			
N-acetyl of GlcNAc[b]					
I	2.048	2.048	2.049	2.053	2.048
II					2.045
IV			2.078	2.081	2.075
V	2.011	2.018	2.010	2.025	2.003
VI	2.090	2.085	2.090 (2.078)[d]	2.081	2.078
N-acetyl of NeuNAc	2.030	2.040	2.034 (trace)		

[a] Chemical shift is obscured by HDO peak. [b] GlcNAc and Gal residues are identified by the following formula by the number in parentheses:

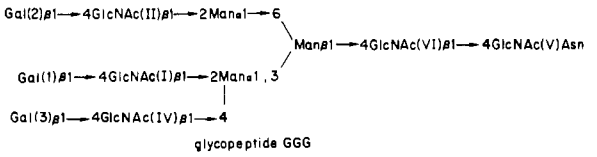

GlcNAc III is the "bisecting GlcNAc" linked β1→4 to the Manβ1→4 residue. This residue has been omitted from the table as the characteristic signals for this residue (Carver et al., 1981; Grey et al., 1982) were absent from the spectra of the glycopeptides. [c] Numbers in parentheses are the $J_{1,2}$ coupling constants in megahertz. [d] Chemical shifts for the non-fucosylated species present in the sample. [e] Chemical shifts published by Vliegenthart et al. (1981).

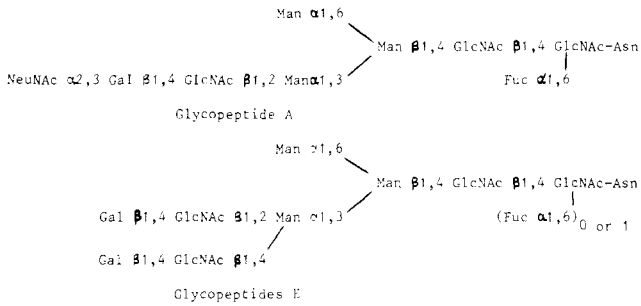

FIGURE 6: Structures of Ric^{R}21 glycopeptides A and E.

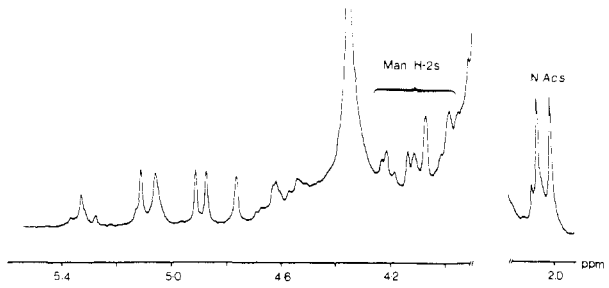

FIGURE 7: The 500-MHz ^{1}H NMR spectrum of Ric^{R}21 glycopeptide fraction B at 70 °C.

(0.014 ppm) and the H-2 signal (0.111 ppm) of Manα1→3 (at 70 °C), compared to the glycopeptide MM. These are characteristic chemical shifts (Grey et al., 1982; Vliegenthart et al., 1983) indicating that the Manα1→3 residue is substituted at position C-2 by a GlcNAc residue. As there is only one arm GlcNAc residue in the glycopeptide, the Manα1→6 residue therefore must be in a terminal position. This is supported by the observed chemical shift for the H-1 signal of the Manβ1→4 residue at its unperturbed chemical shift of 4.771 ppm (70 °C), as substitution of the Manα1→6 residue by a GlcNAc residue would have resulted in an upfield shift of −0.012 ppm for this signal. The broad signal at 4.089–4.129 ppm integrates as three protons, two of which can be identified as H-5 of Fuc and H-3 of Gal.

The chemical shifts of the NeuNAc H-3 signals [H-3(a) at 1.799 ppm and H-3(e) at 2.756 ppm] are characteristic (Vliengenthart et al., 1983) of an α2→3 linkage to galactose. No signals were observed at 2.669 and 1.718 ppm, indicating the absence of any α2→6NeuNAc linkage. Substitution of a terminal galactosyl residue with an α2→3NeuNAc residue is known to result in major perturbations of both the H-1 signal (0.076 ppm) and H-3 signal (0.453 ppm) of galactose (Vliegenthart et al., 1983). These effects are readily apparent in the spectrum of glycopeptide A; the H-1 signal of galactose (4.548 ppm, 22 °C) is downfield by 0.082 ppm compared to an unsubstituted galactose (Vliegenthart et al., 1983), and the H-3 signal of galactose is observed downfield at 4.089–4.129 ppm. Broad signals underneath the NeuNAc H-3(e) signal (from 2.7 to 2.8 ppm) can be assigned to the Asn β-CH_2 protons.

The presence of a Fucα1→6 residue on the asparagine-linked GlcNAc residue is shown by the H-1 signal of Fuc at 4.870 ppm ($J_{1,2}$ = 3.8 Hz), the CH_3 signal of Fuc at 1.200 ppm, and the H-5 signal of Fuc at 4.089–4.129 ppm. Also, the H-1 signal of the core GlcNAc at 4.683 ppm is typical of a fucosylated glycopeptide. Therefore, the structure of the major component of this fraction (glycopeptide A) is a sialylated, fucosylated Man_3 hybrid, as shown in Figure 6. There is clearly some heterogeneity in the peptide moiety of fraction A as shown by the amino acid analysis and reflected in the NMR spectra: small signals are observed at 0.95 ppm and from 1.28 to 1.42 ppm from aliphatic signals in amino acids other than Asn. This heterogeneity could explain the broad signals seen for the H-1 signal of Asn–GlcNAc and the extra shoulder on the fucose CH_3 signal.

Structure of Ric^{R}21 Fraction B Glycopeptides. Glycopeptide fraction B is the neutral glycopeptide fraction that did not absorb onto DEAE-Sephacel. The 500-MHz proton NMR spectrum (at 70 °C) of this fraction is shown in Figure 7, and the chemical shifts obtained for the major species at both 22 and 70 °C are given in Table II.

The ratios of the intensities for the major anomeric hydrogen signals are as follows: 0.7, 1.2, 2, 1, 1, 1, and 1. On the basis

Table II: Chemical Shifts (ppm) of Glycopeptide Protons Derived from High-Resolution NMR Spectroscopy

	glycopeptide B[a]		ovalbumin Man_6 glycopeptide[e]	
protons	22 °C	70 °C	23 °C	75 °C
H-1 of Man[d]				
β1→4 i	*b*	4.768	4.772	4.765
α1→3 i	5.349	5.338	5.348	5.336
α1→6 i	4.870	4.880	4.871	4.883
α1→2 t	5.051	5.060	5.053	5.069
α1→3 t	5.091	5.119	5.089	5.126
α1→6 t	4.908	4.918	4.909	4.920
H-2 of Man[d]				
β1→4 i	4.237	4.213	4.234	4.215
α1→3 i	4.114	4.114	4.114	4.119
α1→6 i	4.147	4.136	4.146	4.126
α1→2 t	4.068	4.073	4.063	4.074
α1→3 t	4.068	4.073	4.063	4.074
α1→6 t	3.986	3.986	3.988	3.985
H-1 of GlcNAc				
core	4.602	4.622	4.601	4.638
Asn linked	5.06[c]	5.06[c]	5.07[c]	5.068
N-acetyl of GlcNAc				
core	2.062	2.066	2.059	2.063
Asn linked	2.009	2.016	2.011	2.022

[a] Chemical shifts are for the major species only. [b] Resonance obscured by the HDO peak. [c] Resonance obscured by other signals. [d] The number refers to the linkage; i indicates internal (i.e., substituted), and t indicates terminal residue (i.e., not substituted). [e] Chemical shifts published by Carver et al. (1981).

of published chemical shifts for the high-mannose glycopeptides (Carver et al., 1981; Vliegenthart et al., 1983), these H-1 signals (at 70 °C) are identified as follows: 0.7 residue of internal α3-linked mannose (5.338 ppm); 1.2 residues of terminal α3-linked mannose (5.119 ppm); 1 residue of terminal α2-linked mannose (5.060 ppm); 1 residue of Asn-linked GlcNAc also at 5.06 ppm; 1 residue of terminal α6-linked mannose (4.918 ppm); 1 residue of internal α6-linked mannose (4.880 ppm); 1 residue of internal β4-linked mannose (4.768 ppm); 1 residue of core GlcNAc (4.662 ppm). Therefore, the major species of fraction B contains six mannose residues. Also included in Table II are the chemical shifts published by Carver et al. (1981) for the $Man_6GlcNAc_2Asn$ glycopeptide derived from ovalbumin. The structure of this ovalbumin Man_6 species is as follows:

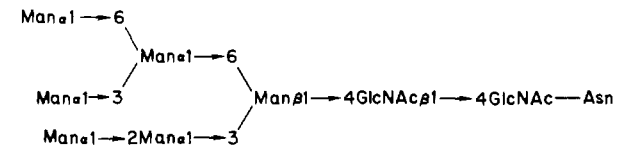

where the single Manα1→2 residue is linked to the lower Manα1→3 arm. The H-1 and H-2 chemical shifts for the mannose residues of the Man_6 species of fraction B are identical with those observed for this ovalbumin

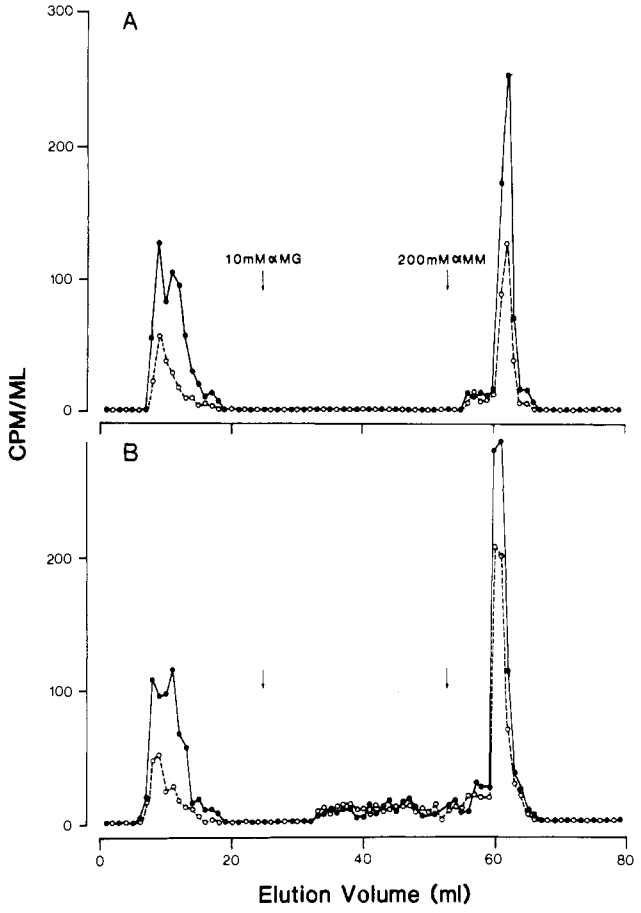

FIGURE 8: Analytical chromatography of glycopeptide fractions D1 and D2 on lentil lectin–Sepharose. The $^3H/^{14}C$ glycopeptide fractions were chromatographed on a column (0.9 × 12 cm) of lentil lectin–Sepharose under the conditions indicated in Figure 4. The arrows indicate the start of elution with 10 mM methyl α-D-glucoside (αMG) and 200 mM methyl α-D-mannoside (αMM), respectively. Fraction size was 1 mL. (A) Glycopeptide fraction D1. Load was 1469 cpm of ^3H and 623 cpm of ^{14}C, and recovery from the column was 87 and 94%, respectively. (B) Glycopeptide fraction D2. Load was 1574 cpm of ^3H and 1206 cpm of ^{14}C, and recovery from the column was 100 and 97%, respectively. (●) ^3H radioactivity; (○) ^{14}C radioactivity.

$Man_6GlcNAc_2Asn$ glycopeptide. Additional support for this Man_6 structure in fraction B comes from endoglycosidase D treatment. The $^{14}C/^3H$-labeled products obtained from the incubation of fraction B with endo D were analyzed on Con A–Sepharose. Only 9% of the ^{14}C label (representing the released Asn[^{14}C]GlcNAc) was unbound on Con A–Sepharose. The remainder of the ^{14}C label and virtually all of the ^3H label eluted in the bound fraction. Assuming equal ^{14}C labeling of the AsnGlcNAc and core GlcNAc residues, this represents 18% cleavage of fraction B glycopeptides under conditions where >80% of $Man_5GlcNAc_2Asn$ was cleaved. This resistance of fraction B to endo D confirms the position of the Manα1→2 residue on the lower Manα1→3 arm. As expected, fraction B was susceptible to endoglycosidase H treatment; analysis of the $^3H/^{14}C$-labeled products by Con A–Sepharose showed >80% cleavage of fraction B.

From the NMR spectrum, the internal Manα3 residue integrates as approximately 0.7 residue, indicating that the $Man_6GlcNAc_2Asn$ glycopeptide represents 70% of the total fraction. The presence of 1.2 residues of terminal α1→3-linked mannose, along with integral values for the other mannose residues, suggests that about 20% of this fraction represents $Man_5GlcNAc_2Asn$. This is consistent with the cleavage of 18% of fraction B with endo D. In addition, there may also be small amounts (~10%) of high-mannose glycopeptides larger than

Table III: Chemical Shifts (ppm) of Glycopeptide Protons Derived from High-Resolution NMR Spectroscopy

protons	glycopeptide C1 at 70 °C	glycopeptide C2 at 70 °C
H-1 of Man[a]		
β1→4 i	4.772	4.772
α→3 i	5.136	5.338
α1→6 i		4.880
α1→2 t		5.066
α1→3 t		5.119
α1→6 t	4.919	4.919
H-2 of Man[a]		
β1→4 i	4.228	4.216
α1→3 i	4.186	4.112
α1→6 i		4.142
α1→2 t		4.073
α1→3 t		4.073
α1→6 t	?	3.983
H-1 of GlcNAc[b]		
I	4.595	
V	5.047	5.047
VI	4.629	4.629
H-1 of Gal	4.537	
H-3(a) of NeuNAc	1.785	
H-3(e) of NeuNAc	2.761	
N-acetyl of GlcNAc[b]		
I	2.048	
V	2.016	2.016
VI	2.075	2.064
N-acetyl of NeuNAc	2.040	

[a] See Table II legend for terminology. [b] See Table I legend for terminology.

Man_6 species. Any non-sialylated Con A binding hybrid glycopeptide would also be included in this fraction. The NMR spectrum shows that, at most, there is only about 10% of an *N*-acetyllactosamine-type glycopeptide present. This is suggested by a small H-1 signal at 5.138 ppm and H-2 signal at 4.188 ppm, indicative of a Manα1→3 residue substituted by a GlcNAcβ1→2 residue, a small *N*-acetyl signal at 2.087 ppm characteristic of a core GlcNAc residue from a $Man_3GlcNAc_2Asn$ species, and small signals in the H-1 region of Gal and arm GlcNAc residues. The complete structure of this minor species, however, cannot be deduced.

Structure of Fraction C Glycopeptides. Analytical chromatography of the DEAE-bound fraction D1 on lentil–Sepharose (Figure 8A) results in an unbound fraction that eluted as two distinct peaks of ^3H radioactivity. The first peak eluted with the column volume while the second peak, with a higher $^3H/^{14}C$ ratio, was slightly retarded on the lentil–Sepharose column. Glycopeptide fraction C is the total lentil-unbound material from the major peak of DEAE-bound glycopeptides. As indicated by the analytical lentil–Sepharose chromatography, 500-MHz NMR analyses of fraction C showed it was a mixture of two major species, fractions C1 and C2 in the approximate ratio 3:7. The chemical shifts of glycopeptide C1 (at 70 °C) (Table III) are identical with those of glycopeptide A except for the absence of a fucose residue. (The H-1 resonance for fucose was obscured by the signals from glycopeptide C2; however, there was no CH_3 signal for fucose at 1.20 ppm, and the H-1 and *N*-acetyl signals of the core GlcNAc are indicative of a non-fucosylated species.) The absence of a fucose residue in glycopeptide C1 is consistent with its behavior on lentil–Sepharose, as non-fucosylated glycopeptides do not bind to lentil–Sepharose (Kornfield et al., 1981).

The chemical shifts of glycopeptide C2 (at 70 °C) (Table III) are identical with those for the $Man_6GlcNAc_2Asn$ glycopeptide B. The presence of high-mannose glycopeptides in this "acidic" fraction could be due to either peptide hetero-

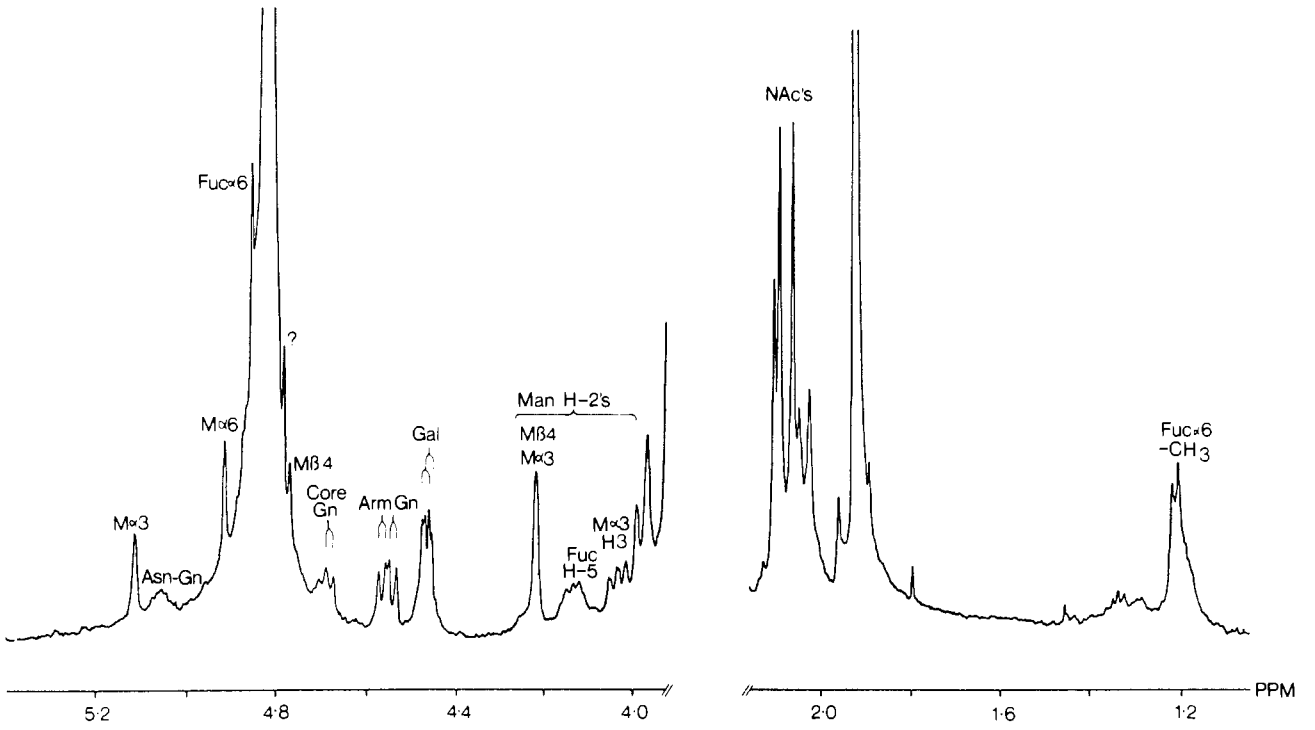

FIGURE 9: The 500-MHz ^1H NMR spectrum of glycopeptide fraction E at 22 °C.

geneity or the presence of phosphorylated mannose residues (Varki & Kornfield, 1980). Treatment of glycopeptide fraction C with endo H for 48 h followed by rechromatography on the DEAE-Sephacel column resulted in all the ^3H radioactivity binding to the ion-exchange column and eluting as a single peak. Therefore, the charge of this high-mannose glycopeptide is not due to the peptide moiety.

Glycopeptide Fraction D2. This material bound to the DEAE column but eluted as a trailing shoulder from the main peak (Figure 3). Analytical chromatography of this fraction on lentil–Sepharose (Figure 8B) showed a similar profile as the major DEAE-bound fraction (Figure 8A), except that a greater percentage of fraction D2 (77% compared to 58%, based on ^{14}C radioactivity) bound to the column. The 500-MHz NMR spectroscopy showed the major species of fraction D2 to be identical with glycopeptide A (results not shown) with a small amount of high-mannose glycopeptides also present. Amino acid analysis of fraction D2 showed a higher peptide content (12.9 nmol of amino acids/nmol of glycopeptide) than glycopeptide A (3.7 nmol of amino acids/nmol of glycopeptide), and this additional peptide moiety is likely to be responsible for the heterogeneity displayed by this sialylated Man_3 hybrid glycopeptide on the DEAE column.

Con A Unbound Ric^{R}21 N-Glycans. Glycopeptide Fraction E. The fraction from the Pronase digest that did not bind to Con A–Sepharose is a mixture of *N*-glycans, and peptides. It has been shown previously (Hughes et al., 1983) that the Ric^{R}21 Con A unbound *N*-glycans show sialic acid heterogeneity. To simplify the purification of these *N*-glycans, therefore, the sample was treated with neuraminidase to remove the sialic acid. The desialylated Con A unbound fraction was redigested with Pronase to reduce any peptide heterogeneity and then subjected to high-voltage electrophoresis in 1% sodium borate. Only a single major $^3H/^{14}C$-labeled peak (glycopeptide fraction E) was obtained, which migrated about 16 cm from the origin under conditions described under Methods. The recovered fraction represents 53% of the ^{14}C radioactivity and 56% of the ^3H radioactivity in the total asialo Con A unbound fraction.

The NMR spectrum, at 22 °C, of glycopeptide fraction E is shown in Figure 9, and the chemical shifts at both 22 and 70 °C are shown in Table I. There are two *N*-acetyllactosaminyl branches present in this glycopeptide as the H-1 signals, for both galactose (4.469 and 4.666 ppm) and GlcNAc (4.564 and 4.542 ppm), integrate to two hydrogens. For comparison, the chemical shifts obtained at 23 °C for the sialic acid free triantennary complex glycopeptide (non-fucosylated) GGG (structure shown in footnotes to Table I) published by Vliegenthart et al. (1981) are also included in Table I. The set of chemical shifts obtained for glycopeptide E are characteristic of a glycopeptide with two complex antennae linked $\beta1\rightarrow2$ and $\beta1\rightarrow4$ to the Man$\alpha1\rightarrow3$ arm. Comparison with glycopeptide A shows differences in the H-2 signal of Man$\alpha1\rightarrow3$ (0.027 ppm) and Man$\beta1\rightarrow4$ (−0.036 ppm), which now coincide at 4.220 ppm; also, the H-3 signal of Man$\alpha1\rightarrow3$ has been resolved from the bulk of the protons at 4.044 ppm. These are diagnostic perturbations resulting from the presence of an additional antenna linked $\beta1\rightarrow4$ to the Man$\alpha1\rightarrow3$ arm of the core (Vliegenthart et al., 1983; compare with glycopeptide GGG). Also characteristic for this antenna is the *N*-acetyl signal of the arm GlcNAc at 2.078 ppm.

As there are only two *N*-acetyllactosamine groups present in glycopeptide E, the Man$\alpha1\rightarrow6$ residue must be unsubstituted. This is confirmed by the upfield position of the H-2 signal of the Man$\alpha1\rightarrow6$ residue at <4.0 ppm (the signal at 4.136 ppm integrates as 0.7 residue and therefore represents only the H-5 signal of fucose—see below) and the downfield position of the H-1 signal of the Man$\beta1\rightarrow4$ residue (0.014 ppm) compared to glycopeptide GGG (Table I), these shifts being typical of a terminal Man$\alpha1\rightarrow6$ residue (Grey et al., 1982; Vliegenthart et al., 1983). There is again some heterogeneity in the peptide moiety; this is indicated by the presence of amino acid signals in the region 1.28–1.45 ppm and from amino acid analysis.

Glycopeptide E is partially (70%) fucosylated as the H-1 and H-5 signals of fucose integrate as 0.7 residue. The observed resonances for the H-1 signal (4.853 ppm), H-5 signal at 4.136 ppm, $-CH_3$ group at 1.211 ppm, and the H-1 and

Table IV: Yields of Ric^{R}21 *N*-Glycans[a]

	glycopeptide	yield (nmol)	% of total recovered glycopeptides
	Hybrid		
Con A bound	sialylated fucosylated hybrid	175	33
	sialylated hybrid (non-fucosylated)	31	6
	neutral hybrid	≤13	≤2
Con A unbound	branched hybrid (fucosylated)	80	15
	branched hybrid (non-fucosylated)	35	7
	High Mannose		
	neutral high-mannose glycopeptides	135	26
	"acidic" high-mannose glycopeptides	55	11

[a] The amounts of each glycopeptide were calculated on the basis of the GlcNAc content, determined by amino acid analysis and the known structures of each fraction.

N-acetyl signals of the core GlcNAc are all characteristic of a Fucα1→6 residue on the asparagine-linked GlcNAc. Additional signals were also observed for the non-fucosylated species, namely, the H-1 signal of the core GlcNAc at 4.622 ppm (at 70 °C) and the *N*-acetyl signal of the core GlcNAc at 2.078 ppm (at 70 °C). The structure of glycopeptide E is shown in Figure 6.

Relative Amounts of N-Glycan Structures in Ric^{R}21 Cells. Table IV summarizes the yields obtained for the Ric^{R}21 N-linked glycopeptides. The amounts were calculated on the basis of the GlcNAc content, determined by amino acid analysis and the known structure(s) of each fraction. The relative amounts should be considered as approximate due to selective losses of glycopeptides during fractionation.

Discussion

The study of lectin-resistant cell lines has proved to be valuable in the understanding of the biosynthetic pathway and the functional significance of glycosylation (Stanley, 1980; Briles, 1982). Previous work in this laboratory (Hughes et al., 1983) using indirect glycopeptide structural analysis suggested that the ricin-resistant BHK cell line Ric^{R}21 has a novel defect in *N*-glycan synthesis resulting in the accumulation of hybrid-type oligosaccharides. However, the structural information obtained was incomplete and furthermore could only partially explain the poor ricin binding behavior of these cells. Therefore, a more comprehensive analysis has been carried out with 500-MHz ^{1}H NMR spectroscopy, and this paper presents the structures of all the major *N*-glycans of Ric^{R}21. This study shows definitively that Ric^{R}21 synthesizes only hybrid and high-mannose *N*-glycans.

The structures of the Ric^{R}21 hybrid *N*-glycans allow a number of important conclusions to be made. First, the hybrid structures contain only three mannose residues. This indicates that the processing of $GlcNAc_1Man_5GlcNAc_2$ by α-mannosidase II (Tabas & Kornfeld, 1978; Harpaz & Schachter, 1980b) to generate $GlcNAc_1Man_3GlcNAc_2$ (MGn) is normal in Ric^{R}21 cells. This mutant, therefore, is defective in the initiation of the complex antenna on the Manα1→6 arm. The glycosyltransferase activity responsible for the initiation of this complex antenna is GlcNAc-transferase II (Harpaz & Schachter, 1980a; Oppenheimer et al., 1981). The GlcNAc-transferase II activity in Ric^{R}21 has been shown to be reduced to 17–27% of the activity of normal BHK cells, as measured in vitro with exogenous substrates (Vischer & Hughes, 1981; Narasimhan et al., 1984). Although this mutant still has some residual GlcNAc-transferase II activity, the *N*-glycan structures clearly show that this activity is unable to function in vivo. The reason for this biosynthetic defect is not clear. One possibility is that the GlcNAc-transferase II in Ric^{R}21 may not be correctly located within the cell, as suggested by Narasimhan et al. (1984). Alternatively, the enzyme may not be able to act in situ due to an alteration in conformation and is active, or partialy active, only after extraction with detergent, which is a requirement for the in vitro assays. A third possibility, which was previously proposed by Hughes et al. (1983), is that the reduced GlcNAc-transferase II activity may result in a dramatic shift in the biosynthetic pathway due to competition between galactosyltransferase and GlcNAc-transferase II, in vivo, for the common oligosaccharide substrate MGn. Significantly, the addition of galactosyl residues to the terminal GlcNAc residue of MGn prevents the action of GlcNAc-transferase II (Vella et al., 1984) and would result inthe synthesis of hybrid oligosaccharides. For this mechanism to operate, both transferases would have to be present in the same compartment of the Golgi. However, recent studies on the subfractionation of the Golgi from Chinese hamster ovary (CHO) cells have shown that the galactosyltransferase activity could be partially resolved from the GlcNAc-transferase II activity, suggesting these transferases reside in different Golgi cisternae (Dunphy & Rothman, 1983).

A number of other lectin-resistant cell lines have also been isolated that show defects in specific glycosyltransferase reactions in vivo yet fail to show a deletion of an enzyme as measured by in vitro assays. For example, the pea lectin resistant mutant, PHA^{R}1.8 PL^{R}7.2 is unable to synthesise core fucosylated *N*-glycans, yet the relevant enzymes appear to be present in at least normal levels (Reitman et al., 1980).

The Ric^{R}21 *N*-glycans do not contain a "bisecting" GlcNAc residue linked to the Manβ1→4 residue. The absence of this residue is significant as many of the hybrid structures described to date contain a bisecting GlcNAc residue (Tai et al., 1977). This residue is inserted by GlcNAc-transferase III (Narasimhan, 1982) and is known to prevent the action of both processing mannosidase II and GlcNAc-transferase II (Schachter et al., 1983), thereby resulting in the synthesis of hybrid *N*-glycans. GlcNAc-transferase III activity could not be detected in either parental BHK cells or Ric^{R}21 cells (Narasimhan et al., 1984); therefore, the absence of this residue in the Ric^{R}21 *N*-glycans is not surprising.

Another very significant finding was that the majority (≥95%) of the unbranched hybrid (MS) was sialylated, and the sialic acid residues exclusively linked α2→3 to galactose. Baenziger & Fiete (1979) have shown that ricin is able to bind to α2→6-substituted galactosyl residues but is unable to bind to α2→3-substituted galactosyl residues. The nature of the sialic acid linkage in the unbranched hybrid therefore explains the very poor ricin binding properties of these cells. The desialylated Con A unbound *N*-glycan is a hybrid structure containing two complex antennae (Figure 6). Earlier work showed this fraction to be extensively sialylated (Hughes et al., 1983), and it seems likely that α2→3 linkages will predominate in this structure also.

Normal BHK cells are known to synthesise complex *N*-glycans bearing both α2→6 and α2→3 sialic acid linkages (van Halbeek et al., 1983; H. van Halbeek, personal communica-

tion). Why does the Ric^{R}21 hybrid structure then contain only $\alpha2\rightarrow3$ sialic acid linkages? The total sialyltransferase activity in Ric^{R}21 cells is the same as that of parental BHK cells (Vischer & Hughes, 1981); therefore, the absence of $\alpha2\rightarrow6$-linked sialic acid residues in the hybrid *N*-glycans is probably not due to an altered $\alpha2\rightarrow6$ sialyltransferase level. It should be stressed, however, that the $\alpha2\rightarrow3$ and $\alpha2\rightarrow6$ sialyltransferase levels have not been quantitated individually. The presence of only $\alpha2\rightarrow3$ sialyl residues in the hybrid may reflect differences in the substrate specificities of the two sialyltransferases. There is some experiment support for this suggestion, as Bendiak & Cook (1983) have shown that the $\alpha2\rightarrow6$ sialyltransferase from embryonic chicken liver exhibited a marked preference for multiantennary acceptors with terminal galactosyl residues; oligosaccharides bearing only one Gal$\beta1\rightarrow4$GlcNAc terminus were found to be relatively poor acceptors. The relative activities of the two enzymes with hybrid *N*-glycan substrates, therefore, warrants further investigation.

Hybrid *N*-glycans have been shown to accumulate in the presence of the glycosylation inhibitor swainsonine (Gross et al., 1983; Kang & Elbein, 1983; Tulsiani & Touster, 1983; Arumugham & Tanzer, 1983) due to the inhibition of the processing α-mannosidase II (Tulsani et al., 1982). In contrast to the hybrid *N*-glycans here, these hybrid structures contain five mannose residues. Some of these hybrid structures were shown to be sialylated (Kang & Elbein, 1983; Tulsiani & Touster, 1983). Sialylated hybrid structures have also been found in P388D mouse macrophage-like cell glycoproteins (Varki & Kornfeld, 1983), as well as the glycoproteins from Prague C Rous sarcoma virus (Hunt & Wright, 1981) and avian myeloblastosis associated virus (Hunt & Wright, 1983). However, the sialic acid linkages in these hybrid structures have not been established. In the light of the current findings, it will be of interest to investigate the sialic acid linkages of these other hybrid *N*-glycans. A structure similar to the Ric^{R}21 branched hybrid (MGG) glycopeptide (Figure 6) was reported for the first time only very recently, being found in the *N*-glycans of human chorionic gonadotropin obtained from a patient with choriocarcinoma (Mizuochi et al., 1983).

Another interesting feature of the Ric^{R}21 *N*-glycans is the predominance of the $Man_6GlcNAc_2$ species in the high-mannose fraction. This could represent mature high-mannose membrane glycoproteins and/or intermediates in the biosynthetic pathway. It is relevant to note that a recent study of the biosynthesis and processing of the *N*-glycans of secreted IgA from MOPC 315 murine plasmacytoma cells showed that the major oligosaccharide that accumulated intracellularly was also $Man_6GlcNAc_2$ (Hickman et al., 1984). The accumulation of $Man_6GlcNAc_2$ species in Ric^{R}21 is unlikely to represent a biosynthetic defect as the high-mannose *N*-glycan content of these cells is identical with that of normal BHK cells (Hughes et al., 1983). The structures of the high-mannose *N*-glycans from parental BHK cells are currently being investigated.

In conclusion, the characterization of the *N*-glycans of this ricin-resistant mutant clearly shows the structural basis for the altered ricin binding properties, and hence resistance, displayed by these cells. This study also shows the feasibility of NMR structural analysis of the *N*-glycans derived from cultured cells.

ACKNOWLEDGMENTS

We thank Gary Mills for growing the Ric^{R}21 cells, Dr. H. Schachter and Stephen Allen for the generous gift of $Man_5GlcNAc_2Asn$ glycopeptide, Drs. J. Carver, H. van Halbeek, J. Kamerling, and H. Schachter for helpful comments, and Lydia Pearson for typing the manuscript. The NMR spectra were recorded on the Bruker AM500 at the Biomedical NMR Centre, National Institute for Medical Research, London, U.K.

REFERENCES

Arumugham, R. C., & Tanzer, M. L. (1983) *J. Biol. Chem. 258*, 11883–11889.

Baenziger, J. U., & Fiete, D. (1979) *J. Biol. Chem. 254*, 9795–9799.

Bendiak, B., & Cook, M. W. (1983) *Biochem. J. 213*, 253–260.

Briles, E. B. (1982) *Int. Rev. Cytol. 75*, 101–165.

Carver, J. P., Grey, A. A., Winnik, F. M., Hakimi, J., Ceccarini, C., & Atkinson, P. H. (1981) *Biochemistry 20*, 6600–6606.

Dubois, M., Gilles, K. A., Hamilton, J. K., Rebers, P. A., & Smith, F. (1956) *Anal. Chem. 28*, 350–356.

Dunphy, W. G., & Rothman, J. E. (1983) *J. Cell Biol. 97*, 270–275.

Finne, J., & Krusius, T. (1982) *Methods Enzymol. 83*, 269–277.

Grey, A. A., Narasimhan, S., Brisson, J.-R., Schachter, H., & Carver, J. P. (1982) *Can. J. Biochem. 60*, 1123–1131.

Gross, V., Tran-Thi, T.-A., Vosbeck, K., & Heinrich, P. C. (1983) *J. Biol. Chem. 258*, 4032–4036.

Harpaz, N., & Schachter, H. (1980a) *J. Biol. Chem. 255*, 4885–4893.

Harpaz, N., & Schachter, H. (1980b) *J. Biol. Chem. 255*, 4894–4902.

Hickman, S., Theodorakis, J. L., Greco, J. M., & Brown, P. H. (1984) *J. Cell Biol. 98*, 407–416.

Hughes, R. C., & Mills, G. (1983) *Biochem. J. 211*, 575–587.

Hughes, R. C., Mills, G., & Stojanovic, D. (1983) *Carbohydr. Res. 120*, 215–234.

Hunt, L. A., & Wright, S. E. (1981) *J. Virol. 39*, 646–650.

Hunt, L. A., & Wright, S. E. (1983) *J. Virol. 45*, 233–240.

Kang, M. S., & Elbein, A. D. (1983) *J. Virol. 46*, 60–69.

Kornfeld, K., Reitman, M. L., & Kornfeld, R. (1981) *J. Biol. Chem. 256*, 6633–6640.

Krusius, T., Finne, J., & Rauvala, H. (1976) *FEBS Lett. 71*, 117–120.

Meager, A., Ungkitchanukit, A., & Hughes, R. C. (1976) *Biochem. J. 154*, 113–124.

Mizuochi, T., Nishimura, R., Derappe, C., Taniguchi, T., Hamomoto, T., Mochizuki, M., & Kobata, A. (1983) *J. Biol. Chem. 258*, 14126–14129.

Narasimhan, S. (1982) *J. Biol. Chem. 257*, 10235–10242.

Narasimhan, S., Wilson, J. R., Martin, E., & Schachter, H. (1979) *Can. J. Biochem. 57*, 83–96.

Narasimhan, S., Harpaz, N., Longmore, G., Carver, J. P., Grey, A. A., & Schachter, H. (1980) *J. Biol. Chem. 255*, 4876–4884.

Narasimhan, S., Allen, S., Hughes, R. C., & Schachter, H. (1984) *Glycoconjugates J. 1*, 51–62.

Ogata, S. I., Muramatsu, T., & Kobata, A. (1975) *J. Biochem. (Tokyo) 78*, 687–696.

Oppenheimer, C. L., Eckhardt, A. E., & Hill, R. L. (1981) *J. Biol. Chem. 256*, 11477–11482.

Reitman, M. L., Trowbridge, I. S., & Kornfeld, S. (1980) *J. Biol. Chem. 255*, 9900–9906.

Rosen, S. W., & Hughes, R. C. (1977) *Biochemistry 16*, 4908–4915.

Schachter, H., Narasimhan, S., Gleeson, P., & Vells, G. (1983) *Can. J. Biochem. Cell Biol. 61*, 1049–1066.

Stanley, P. (1980) in *The Biochemistry of Glycoproteins and Proteoglycans* (Lennarz, W. J., Ed.) pp 161–189, Plenum Press, New York.
Tabas, I., & Kornfeld, S. (1978) *J. Biol. Chem. 253*, 7779–7786.
Tai, T., Yamashita, K., Ito, S., & Kobata, A. (1977) *J. Biol. Chem. 252*, 6687–6694.
Tulsiani, D. R. P., & Touster, O. (1983) *J. Biol. Chem. 258*, 7578–7585.
Tulsiani, D. R. P., Harris, T. M., & Touster, O. (1982) *J. Biol. Chem. 257*, 7936–7939.
van Halbeek, H., van Beek, W. P., Blanken-Aarsen, G. J., & Vliengenthart, J. F. G. (1983) in *Proceedings of the International Symposium on Glycoconjugates, 7th* (Chester, M. A., Heinegard, D., Lundblad, A., & Svensson, S., Eds.) pp 864–865, Rahms i Lund, Sweden.
Varki, A., & Kornfeld, S. (1980) *J. Biol. Chem. 255*, 10847–10858.
Varki, A., & Kornfeld, S. (1983) *J. Biol. Chem. 258*, 2808–2818.
Vella, G., Paulsen, H., & Schachter, H. (1984) *Can. J. Biochem. Cell Biol. 62*, 409–417.
Vischer, P., & Hughes, R. C. (1981) *Eur. J. Biochem. 117*, 275–284.
Vliengenthart, J. F. G., van Halbeek, H., & Dorland, L. (1981) *Pure Appl. Chem. 53*, 45–77.
Vliegenthart, J. F. G., Dorland, L., & van Halbeek, H. (1983) *Adv. Carbohydr. Chem. Biochem. 41*, 209–374.

Structures of the Carbohydrate Moieties of Two Monoclonal Human λ-Type Immunoglobulin Light Chains†

Takashi Ohkura, Takashi Isobe,‡ Katsuko Yamashita, and Akira Kobata*

Department of Biochemistry, Kobe University School of Medicine, Chuo-ku, Kobe, Japan
Received July 27, 1984

ABSTRACT: Human Bence Jones proteins of λ type, Wh and Nei, both of which belong to subgroup II, contain an asparagine-linked sugar chain. Their carbohydrate moieties were liberated as oligosaccharides by hydrazinolysis and labeled by reduction with NaB^3H_4 after N-acetylation. Structural studies of each oligosaccharide by sequential exoglycosidase digestion in combination with methylation analysis revealed that Wh λ contains the mono- and disialylated oligosaccharides

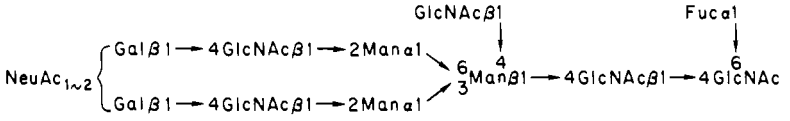

while Nei λ contains the two acidic oligosaccharides

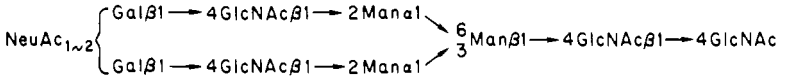

These oligosaccharides are different from the oligosaccharides found in another λ-type Bence Jones protein, Sm λ, by Chandrasekaran et al. [Chandrasekaran, E. V., Mendicino, A., Garver, F. A., & Mendicino, J. (1981) *J. Biol. Chem. 256*, 1549–1555] and Garver et al. [Garver, F. A., Chang, L. S., Kiefer, C. R., Mendicino, J., Chandrasekaran, E. V., Isobe, T., & Osserman, E. F. (1981) *Eur. J. Biochem. 115*, 643–652].

Each of the heavy chains of human immunoglobulin G (IgG) contains an asparagine-linked sugar chain in its Fc portion (Clamp et al., 1964). Although the light chains usually lack carbohydrate, some light chains of human myeloma proteins were reported to contain sugar chains (Abel et al., 1968; Spiegelberg et al., 1970). The structure of the asparagine-linked sugar chain in Sm λ, one such carbohydrate-containing Bence Jones protein, was elucidated as shown in Chart I by Chandrasekaran et al. (1981) and Garver et al. (1981). By comparing the fractionation patterns of oligosaccharides released from 10 different IgG myeloma proteins by Bio-Gel P-4 column chromatography, we found that a variety of oligosaccharide patterns was obtained from these glycoproteins (Mizuochi et al., 1982). The carbohydrate-containing Bence Jones (BJ) proteins were reported to have different sugar contents (Abel et al., 1968; Spiegelberg et al., 1970). In view of recent reports that indicate a functional role

Chart I: Proposed Structures of Sugar Chains Found in BJ Protein, Sm λ, by Chandrasekaran et al. (1981) and Garver et al. (1981)

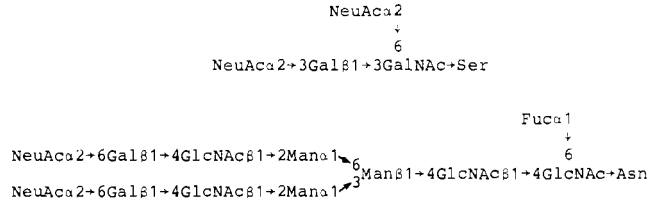

† This work has been supported in part by Grant-in-Aids for Scientific Research, the Ministry of Education, Science and Culture of Japan, and by a research grant from Yamada Science Foundation.
* Address correspondence to this author at the Department of Biochemistry, Institute of Medical Science, University of Tokyo, 4-6-1 Shirokanedai, Minato-ku, Tokyo 108, Japan.
‡ Present address: Department of Medicine, Third Division, Kobe University School of Medicine, Chuo-ku, Kobe 650, Japan.

0006-2960/85/0424-0503$01.50/0